TITLE

Making sense of the linear genome, gene function and TADs

AUTHORS

Helen S Long[1,2], Simon Greenaway[2], George Powell[1,2], Ann-Marie Mallon[2],

Cecilia M Lindgren[3,4,5], Michelle M Simon[2]

AUTHOR AFFILIATIONS

1) Nuffield Department of Medicine, University of Oxford, United Kingdom
2) MRC Harwell, MGU, Didcot, United Kingdom
3) Wellcome Centre for Human Genetics, University of Oxford, United Kingdom
4) Big Data Institute, Li Ka Shing Centre for Health Information and Discovery, University of Oxford. Oxford, United Kingdom
5) Medical and Population Genetics Program, Broad Institute of MIT and Harvard, Cambridge, MA, USA.

ABSTRACT

Background: Topologically associating domains (TADs) are thought to act as functional units in the genome. TADs co-localise genes and their regulatory elements as well as forming the unit of genome switching between active and inactive compartments. This has led to the speculation that genes which are required for similar processes may fall within the same TADs, allowing them to share regulatory programs and efficiently switch between chromatin compartments. However, evidence to link genes within TADs to the same regulatory program is limited.

Results: We investigated the functional similarity of genes which fall within the same TAD. To do this we developed a TAD randomisation algorithm to generate sets of “random TADs” to act as null distributions. We found that while pairs of paralogous genes are enriched in TADs overall, they are depleted in TADs with CCCTC-binding factor (CTCF) ChIP-seq peaks at both boundaries. By assessing gene constraint as a proxy for functional importance we found that genes which singly occupy a TAD have greater functional importance than genes which share a TAD, and these genes are enriched for developmental processes. We found little evidence that pairs of genes in CTCF bound TADs are more likely to be co-expressed or share functional annotations than can be explained by their linear proximity alone.

Conclusions: These results suggest that algorithmically defined TADs consist of two functionally different groups, those which are bound by CTCF and those which are not. We detected no association between genes sharing the same CTCF TADs and increased co-expression or functional similarity, other than that explained by linear genome proximity. We do however find that functionally important genes are more likely to fall within a TAD on their own suggesting that TADs play an important role in the insulation of these genes.

KEYWORDS

TADs, topologically associating domains, Hi-C, Chromatin structure, gene regulation, gene function, gene expression

BACKGROUND

The organisation of the mammalian genome in three dimensional space is non-random and hierarchically organised (1). Using Hi-C (2) it was shown that chromosomal loci are clustered into two, mega base scale structures known as the A and B compartments (3). The A compartment is enriched for active, euchromatin whereas the B compartment is enriched for inactive, heterochromatin (3,4). The formation of chromatin compartments is hypothesised to be driven by phase separation (5). By analysing chromatin contact maps at kilobase resolution Dixon et al. were able to identify a finer level of chromatin organisation known as Topologically Associating Domains (TADs). TADs are regions of the genome characterised by a high degree of self-interaction within the length of the TAD, and a low degree of interactions with regions outside of the TAD even if they are a similar distance away (6). TAD boundaries are enriched for CCCTC-binding factor (CTCF) binding sites and are thought to be formed by active loop extrusion, during which DNA is extruded through cohesion (forming a loop) until the extrusion is stalled by a pair convergently orientated CTCF binding sites at the TAD boundaries (5–8). Comparisons of TADs between tissues suggested that they are largely tissue invariant (4,6,9). It has also been proposed that a third category of chromatin organisation exists, which nests within TADs, these ‘sub-TADs’, are formed by the same mechanisms as TADs but have weaker insulation and are more likely to vary depending on the cell type (10). However, it is currently unclear whether sub-TADs constitute functionally different structures to TADs (10).

It has been proposed that TADs constitute functional units in the genome, important for correct regulation of gene expression. TADs co-localise regulatory elements with their target genes, and are thought to promote co-regulation of the genes they contain, creating “gene

65 regulatory domains" (11). By inserting regulatory sensors along the length of the genome
66 Symmons et al. found evidence that the activity of enhancers is split into regulatory
67 domains which highly correlate with TADs (12). This provided experimental evidence that
68 TADs potentially facilitate enhancers to carry out "non-specific" co-regulation of all genes in
69 the TAD (11,12). Simultaneously, TADs are thought to insulate genes from aberrant
70 regulation by regulatory elements outside the TAD (enhancer hijacking) (11). Several
71 examples of congenital disease have been linked to TAD boundary disruptions allowing
72 enhancer hijacking demonstrating that at least in these cases, TAD boundaries are essential
73 for proper gene regulation (13,14). TAD boundaries are also able to block the spread of
74 transcription, and repressive chromatin (11). It has been observed that the unit of
75 compartment switching in the genome tends to be a single or series of TADs (15). Adding to
76 this picture, it has been suggested that genes within the same TAD have highly correlated
77 expression patterns (16–19). This has led to the speculation that genes which are required
78 for specific processes may be contained within the same TAD to allow them to share
79 regulatory programs and efficiently switch between the active and inactive compartments
80 (20). Studies have already indicated that some TADs may be enriched for lineage specific
81 genes (20,21), but the global relationship between TADs and gene function is yet to be fully
82 understood.

83 It has long been known that the linear order of genes in the genome is non-random with
84 respect to gene function. Genes that are close together in linear space are more likely to
85 have correlated expression patterns (22), and share pathways and protein-protein
86 interactions (PPI) (23). Genes within TADs are by definition also close together in the linear
87 genome therefore the linear proximity between genes is an important confounding factor
88 when studying the similarity of genes that share a TAD. It is also possible that the increased

89 similarity of genes that are proximal in the linear order occurs on a similar scale to TADs. By
90 promoting co-regulation of genes, TADs could explain the increased functional similarity
91 between proximal genes.

92 We hypothesised that TADs form functional units and therefore genes within them are more
93 likely to share functional annotations than can be explained by linear proximity alone. In
94 order to test this hypothesis we utilised some of the highest quality mammalian Hi-C data
95 currently in the public domain (24) and annotated TADs using two TAD calling algorithms;
96 Arrowhead and TopDom (23,24). We first assessed the relationship between TADs and gene
97 paralogy as well as constraint. Then, focusing on TADs most likely to have been formed by
98 loop extrusion, we assessed the functional relatedness of non-paralogous protein coding
99 genes within them, using four functional annotations: expression correlation, Gene ontology
100 (GO) semantic similarity, shared pathways and PPI.

101

102 RESULTS

103 Characteristics of TADs in cortical neurons and embryonic stem cells (ESCs)

104 We analysed ESC and cortical neuron Hi-C data from Bonev et al. (24) using the Juicer
105 pipeline (25). This data represents some of the highest quality mammalian Hi-C data
106 currently in the public domain. Throughout this work we have focused on autosomal TADs,
107 so unless explicitly stated TADs refers to autosomal TADs only. We annotated 8371 (median
108 size 0.29Mb) and 16002 (median size 0.11Mb) TADs in ESCs, and 8001 (median size 0.32Mb)
109 and 13835 (median size 0.12Mb) TADs in cortical neurons, using two TAD callers Arrowhead
110 (25) and TopDom (26), respectively (Figure 1A-B). We detected more, but smaller TADs with
111 TopDom than with Arrowhead for both cell types. Our results confirm the finding from

112 Bonev et al. (found using the directionality index TAD calling method) that there are more
113 and smaller TADs in ESCs than cortical neurons (24).

114 To learn more about the distribution of TADs in the genome we looked at their association
115 with chromosomes and protein-coding genes, matching the expected null, we observed
116 that, for both TAD callers and datasets, the number of TADs on a chromosome correlates
117 strongly with the size of the chromosome (Figure 1C) (r range 0.9-0.94).

118 Most TADs contain relatively few genes (mean number of genes: ~2.74 and ~3.49
119 (Arrowhead), and ~0.95 and ~1.08 (TopDom) in ESCs and cortical neurons, respectively) and
120 there is little correlation between the number of genes within a TAD and the TAD size (r
121 range 0.2-0.3) (Figure 1D). We investigated several TADs which contained a large number of
122 genes and found that they contained genes from large paralog families e.g. olfactory genes
123 and protocadherin (Figure 1D). This is consistent with previous studies which have noted
124 that genes from these functional families tend to fall within the same TAD, likely due to
125 their shared regulatory requirements (11).

126

127 **TAD randomisation**

128 In order to globally assess the functional similarity between genes in the same TADs we
129 sought to synthesise “random TADs” representing the null distribution. We developed two
130 randomisation strategies in order to generate two null distributions controlling for different
131 possible confounding signals. In the first randomisation strategy, which we refer to as
132 random TADs, we maintained the basic structure of real TADs i.e. TAD size, number of genes
133 within the TAD and the approximate TAD overlap structure. This allowed us to control for

134 the influence of linear gene order and distance which are known to correlate with gene
135 functional similarity (22,23). In this randomisation strategy, the position of each TAD was
136 randomised within the same chromosome to a new region of the same size, containing the
137 same number of genes as the original TAD. For TopDom random TADs, TAD overlapping was
138 prevented, reflecting the non-overlapping structure of TopDom TADs. For Arrowhead
139 random TADs, if the new random TAD overlapped an existing random TAD this was
140 controlled in order to favour "nested" TADs, thereby approximating the global TAD overlap
141 structure seen in Arrowhead TADs (see Methods) (Figure 2B, Figure 3A). In the second
142 randomisation method, which we refer to as random genome TADs, we again maintained
143 the basic TAD structure but removed signal attributed to the linear gene. In order to do this,
144 the positions of TADs were maintained but the order of the genes in the genome was
145 randomly shuffled within each chromosome (Figure 2C). Using both randomisation
146 strategies allows us to disentangle the functional similarity of genes within the same TAD
147 from the functional similarity which can be attributed to proximity in the linear genome.
148 Each TAD randomisation method was run 100 times for each cell type and each TAD caller.

149 In order to compare the functional similarity of genes within TADs to genes within random
150 TADs/random genome TADs, we adopted a pairwise comparison approach (Figure 2D). For
151 every feature investigated every possible pair of genes within a TAD/random TAD was
152 compared in order to generate a distribution of scores. The distribution of scores for each
153 feature in TADs was compared to each of 100 sets of random TADs and the median p-value
154 was reported.

155 To assess the gene distribution within TADs, we compared the distance between genes in
156 TADs to genes in random TADs. We found that for both TAD callers, and both cell types,

genes are significantly further apart in TADs than in random TADs (Figure 3B, median p-values; Arrowhead ESC vs random TADs: p-value<0.001, Arrowhead cortical neuron vs random TADs: p-value<0.001, TopDom ESC vs random TADs: p-value<0.001, TopDom cortical neuron vs random TADs: p-value<0.001).

It has previously been shown that TAD boundaries are enriched for CTCF which is hypothesised to play a crucial role in TAD formation by loop extrusion (5–8). To assess this in our data we tested for the presence of CTCF ChIP-seq peaks near TAD boundaries vs random TAD boundaries (Figure 3C, Supplementary figure 2). We observed that ~ 62%, 52%, 28%, 28% of ESC Arrowhead TADs, ESC TopDom TADs, cortical neuron Arrowhead TADs and cortical neuron TopDom TADs, respectively, had a CTCF ChIP-seq peak within in ±10kb of both TAD boundaries. This is compared to ~ 29%, 29%, 4.5%, 5.3% of ESC Arrowhead random TADs, ESC TopDom random TADs, cortical neuron Arrowhead random TADs and cortical neuron TopDom random TADs, respectively. Supporting previous reports (4,6,27,28), this suggests that CTCF binding is common at the boundaries of TADs and is more prevalent than expected if TADs were randomly placed. This result also shows that more ESC TADs have a CTCF ChIP-seq peak near both boundaries than cortical neuron TADs. This could be due to a reduction in the number of chromatin domains formed by loop extrusion during differentiation. However, we noted that this still left 30%, 29%, 46%, 38% of ESC Arrowhead TADs, ESC TopDom TADs, cortical neuron Arrowhead TADs and cortical neuron TopDom TADs, respectively, which had a CTCF ChIP-seq near only one boundary and 7.9%, 19%, 27% and 35% of ESC Arrowhead TADs, ESC TopDom TADs, cortical neuron Arrowhead TADs and cortical neuron TopDom TADs, respectively, which did not have a ChIP-seq peak near either boundary. This could suggest that these domains may not be

180 formed by loop extrusion and therefore may not conform to the popular mechanistic
181 definition of TADs (10).

182 In order to assess the features of these TADs separately we split TADs into CTCF TADs (which
183 we define as TADs with a CTCF ChIP-seq peak within ±10kb of both boundaries) and non
184 CTCF TADs (which we define as TADs with a CTCF ChIP-seq peak within ±10kb of one, or
185 neither boundary) (Supplementary figure 2). We compared the size of CTCF TADs and non
186 CTCF TADs between ESCs and cortical neurons. In both CTCF TADs and non CTCF TADs we
187 found cortical neuron TADs were significantly larger (p-value<0.001, except Arrowhead non
188 CTCF TADs which was not significantly different) (Supplementary figure 3A-B). We also
189 compared the distance between genes in CTCF and non CTCF TADs to random CTCF/non
190 CTCF TADs, respectively. We found that genes are significantly further apart in both CTCF
191 TADs and non CTCF TADs than expected in random CTCF/non CTCF TADs (p-value<0.001)
192 (Supplementary figure 3C-D).

193

194 **TADs vs paralogy and gene constraint**

195 We have shown examples of TADs that contain a large number of genes from the same
196 paralogous families (Figure 1D), suggesting that genes within TADs could be more
197 functionally similar due to shared ancestry (29). We therefore investigated whether genes
198 within TADs are enriched for paralogous gene pairs, genome wide. To do this we assessed
199 the proportion of paralogous gene pairs within TADs and random TADs. Similarly to Ibn-
200 Salem et al. (30) we found a greater proportion of paralogous gene pairs fall within TADs
201 compared to random TADs (Figure 4A, median p-value of TADs vs random TADs <0.001).
202 This suggests that pairs of paralogous genes are more likely to fall within the same TAD than

203 can be explained by the linear proximity of the genes alone. We further investigated this
204 relationship and found that TADs which contain at least one pair of paralogs are more likely
205 to be significantly larger in size than TADs with no paralogs (Figure 4B, p-value <0.001).
206 When these TADs are split into CTCF TADs and non CTCF TADs we find that pairs of paralogs
207 are significantly enriched in non CTCF TADs compared to random non CTCF TADs (median p-
208 value of non CTCF TADs vs random non CTCF TADs <0.001). However, the opposite is true
209 for CTCF TADs (median p-value of CTCF TADs vs random CTCF TADs <0.001 for ESC
210 Arrowhead, ESC TopDom and cortical neuron Arrowhead and <0.01 for cortical neuron
211 TopDom) (Supplementary figure 4). This suggests that although pairs of paralogs are
212 enriched in TADs they are depleted in CTCF TADs, which are more likely to be "true" TADs
213 formed by loop extrusion.

214 In order to further assess the impact of evolutionary forces on genes within TADs, we
215 assessed the average constraint scores of genes in TADs. Constraint scores quantify the
216 degree of selective constraint acting on protein coding genes, with a higher score indicating
217 a greater strength of purifying selection (31). Selective constraint can change over
218 evolutionary time, and we therefore considered constraint scores calculated in the mouse
219 lineage (32). For TADs called using Arrowhead, we find that genes which singly occupy a TAD
220 are significantly more constrained than the mean constraint of genes co-occupying TADs
221 (Figure 4C-D). Genes singly occupying an Arrowhead TAD also have significantly higher
222 constraint than seen in random TADs (suggesting the result cannot be explained by the
223 structure of the linear genome alone) or random genome TADs (FDR corrected median p-
224 value of genes singly occupying TADs vs genes singly occupying TADs in random TADs or
225 random genome TADs <0.01, Supplementary figure 5). This suggests that genes, which singly
226 occupy TADs, may be under higher selective constraint and more functionally important

227 than genes which co-occupy a TAD. This might suggest that the protection from aberrant
228 regulation of functionally important genes, implied by being in a private TAD, is under
229 selective constraint. Interestingly, this relationship is not seen for TADs called using TopDom
230 despite the fact that the two TAD callers detect a similar proportion of TAD containing only
231 a single gene (~ 21% and 20% of Arrowhead TADs, and 17% and 20% of TopDom TADs, in
232 ESCs and cortical neurons, respectively). This could be because TopDom TADs contain a
233 much larger percentage of TADs with no genes than Arrowhead TADs (~ 37% and 31% of
234 Arrowhead TADs, and 63% and 57% of TopDom TADs, in ESCs and cortical neurons,
235 respectively). This means that there are far fewer TopDom TADs than Arrowhead TADs
236 which contain more than one gene.

237 We next sought to test if the relationship between Arrowhead TADs and average gene
238 constraint is observable in both CTCF TADs and non CTCF TADs. When considering only
239 Arrowhead CTCF TADs, as seen above, we find that generally the constraint of genes in
240 singly occupied TADs is significantly higher relative to the average constraint of genes co-
241 occupying a CTCF TAD. On the other hand, in Arrowhead non CTCF TADs, we find a weaker
242 relationship between genes singly occupying a non CTCF TAD and constraint
243 (Supplementary figure 6). The difference between CTCF TADs and non CTCF TADs in terms of
244 their enrichment for paralogous gene pairs and their relationship with gene constraint
245 supports the possibility that TADs detected by Arrowhead and TopDom may be made up of
246 two functional groups. As CTCF TADs are bounded by CTCF they are likely to have been
247 formed by the process of loop extrusion and are therefore more likely to be “true TADs”. In
248 contrast, non CTCF TADs may have been formed by other mechanisms (10).

249 In order to assess which biological processes genes which singly occupy an Arrowhead TAD
250 are involved in, we carried out a functional enrichment analysis (see Methods) using
251 Biological process GO terms (Figure 4E). We found that genes which singly occupy an
252 Arrowhead CTCF TAD are highly enriched for developmental processes, genes which occupy
253 a TAD with one other gene (double occupancy) are also enriched for developmental
254 processes but to a lesser extent and genes which occupy a TAD with two other genes (triple
255 occupancy) are less enriched for developmental processes still. For example, "multicellular
256 organism development" is the most significant GO term associated with singly occupied
257 TADs in both ESCs and cortical neurons (p-value= $5.04x10^{-54}$ and $1.13x10^{-48}$, respectively),
258 but it is less significantly associated in doubly occupied or triply occupied TADs (doubly
259 occupied: p-value= $1.55x10^{-23}$ and $7.74x10^{-22}$, triply occupied: p-value= $1.47x10^{-07}$and
260 $8.55x10^{-11}$ for ESC and cortical neuron, respectively). We repeated the enrichment analysis
261 using genes which singly, doubly and triply occupy random Arrowhead TADs in order to
262 establish whether randomly placed TADs with similar features (e.g. only one gene in the
263 length of the TAD) have a similar pattern of enrichment (Supplementary figure 7). We found
264 that genes that singly occupy a random TAD are also enriched for developmental processes
265 but to a lesser degree than Arrowhead TADs. This suggests that the enrichment for
266 developmental function observed in genes that singly occupy an Arrowhead TAD cannot be
267 explained by the linear genome alone.

268

269 **Expression and functional similarity of non-paralogous genes in CTCF TADs**

270 We have shown that CTCF TADs and non CTCF are unequal in their functional relevance,
271 hence we decided to focus on the functional similarity of pairs of genes in CTCF TADs, as

272 they are more likely to represent “true” TADs (Figure 2). Since paralogous gene pairs are
273 highly likely to share functional similarity and we have previously assessed their relationship
274 with TADs (Figure 4A-B, Supplementary figure 4) we excluded all pairs of paralogous genes
275 and removed the olfactory genes (see Methods) in all functional analyses. This will allow the
276 assessment of functional similarity between genes within TADs without recent shared
277 ancestry.

278 In order to assess whether pairs of genes in the same TAD have correlated expression
279 patterns we downloaded FPKM counts from RNA-seq expression data. RNA-seq generated
280 during neural differentiation from Bonev et al. (24) and from the most closely matching cell
281 types/tissues to ESCs and cortical neurons which had greater than three samples (mouse
282 ESCs differentiating to primordial germ cell like cells (PGC) and forebrain at different
283 embryonic stages, respectively) from Encode or GEO were used (33–36). Using these
284 expression counts we calculated spearman’s rank correlation coefficient between pairs of
285 genes in CTCF TADs, 100 sets of random CTCF TADs, and 100 sets of random genome CTCF
286 TADs (Figure 5C-D). We found pairs of genes in CTCF TADs have a significantly higher
287 expression correlation than pairs of genes in random genome CTCF TADs in 7 out of 8
288 comparisons (median p-value<0.05). This is an expected result because randomising the
289 genome removes the effect of linear gene proximity. However, in 6 out of 8 comparisons we
290 find no significant difference in expression correlation between pairs of genes in CTCF TADs
291 and pairs of genes in random CTCF TADs (median p-value<0.05). This suggests that contrary
292 to the majority of other studies (16–19) we find little evidence that pairs of genes sharing a
293 TAD are more likely to have similar expression patterns than can be explained by their linear
294 proximity. A study by Soler-Oliva et al. found that algorithmically identified co-expression

295 domains in breast tissue/breast cancer tend not to coincide with TADs, which supports our
296 findings (37).

297 Next, we sought to assess whether pairs of genes within the same CTCF TAD are more likely
298 to share functional annotations than pairs of genes in random CTCF TADs or random
299 genome CTCF TADs. Here, we used molecular function (MF) GO semantic similarity scores,
300 shared pathways, and PPI (see methods). In 11 out of 12 comparisons we found that pairs of
301 genes in CTCF TADs are significantly more similar (median p-value<0.01) in terms of
302 functional annotation than pairs of genes in random genome CTCF TADs (Figure 6D-F).
303 Again, this is expected as randomising the genome removes functional similarity that can be
304 explained by linear proximity. Using binned linear distance, we found greater similarity
305 between pairs of genes which are in very close linear proximity than expected if genes were
306 randomly ordered on the chromosome (Figure 6A-C). We next compared the functional
307 annotations of genes in CTCF TADs with genes in random CTCF TADs. We found that for the
308 majority of comparisons there was no significant difference (8 out of 12 comparisons,
309 median p-value<0.05) (Figure 6D-F). Pairs of genes in Arrowhead ESC CTCF TADs and
310 Arrowhead cortical neuron CTCF TADs have significantly more similar MF GO terms than
311 pairs of genes in random CTCF TADs (median p-value <0.01 and <0.05, respectively). A
312 similar trend in MF GO similarity was observed for all other CTCF TADs compared to random
313 CTCF TADs but the difference wasn't significant in the other 2 comparisons (median p-value
314 <0.05). This could indicate that pairs of genes in CTCF TADs have slightly more similar MF GO
315 term annotations than pairs of genes in random CTCF TADs. However, perhaps this is limited
316 to few TADs as the increase in similarity is very small and often not significant. Pairs of genes
317 in cortical neuron TopDom CTCF TADs are significantly more likely to share a pathway or PPI
318 than pairs of genes in random CTCF TADs (median p-value<0.05). However, the trend in the

319 difference in proportion of gene pairs sharing a pathway or PPI between cortical neuron
320 Arrowhead CTCF TADs and random CTCF TADs is inconsistent and the opposite trend was
321 observed for all ESC CTCF TADs compared to ESC random CTCF TADs. This could suggest a
322 cell type difference in CTCF TAD structure in which pairs of genes sharing a pathway/PPI are
323 more likely to fall within the same CTCF TAD in differentiated cells like cortical neurons
324 compared to undifferentiated cells like ESCs. However, the inconsistency of the results
325 suggests this effect is likely to be small and perhaps driven by few TADs. Overall, we find the
326 biggest contribution to the functional similarity between pairs of genes in CTCF TADs can be
327 attributed to their linear proximity in the genome. When we control for linear proximity we
328 find a less consistent picture but in the majority of comparisons, pairs of genes in CTCF TADs
329 are no more likely to be functionally similar than if CTCF TADs were randomly placed.

330

331 ## DISCUSSION

332 TADs are thought to co-localise regulatory elements and their target genes, insulate genes
333 from off-target enhancer interactions, and block the spread of genome activation (11). Due
334 to these findings we hypothesised that genes sharing a TAD would be more likely to be co-
335 regulated. This is because in the absence of further insulation/specificity, enhancers may be
336 able to “scan” all regulatory elements in the TAD. We hypothesised that if this is the case
337 one might expect genes within TADs to have higher co-expression and greater functional
338 similarity than can be explained purely by the proximity of genes in the linear order of the
339 genome.

340 Similarly to previously described work by Ibn-Salem et al. (30) we found that pairs of
341 paralogous genes are more likely to fall within the same TAD than expected if TADs are

342 randomly placed within chromosomes (Figure 4A). This presents a clear case in which TADs
343 contain functionally similar genes and could reflect the need for paralogs to share
344 regulatory elements. However, we go on to show that TADs can be split into CTCF TADs and
345 non CTCF TADs, and whilst pairs of paralogous genes are more likely to fall within non CTCF
346 TADs than randomly placed non CTCF TADs, paralogous gene pairs are depleted in CTCF
347 TADs (Supplementary figure 4). This suggests that paralogs are depleted in domains formed
348 by loop extrusion which may be more likely to represent 'true' TADs.

349 To further investigate the relationship between gene evolution and TADs, we analysed the
350 average gene constraint of genes sharing TADs. We found that genes which singly occupy a
351 TAD (called by Arrowhead) are statistically more constrained than genes in TADs with
352 multiple genes. This suggests that genes in TADs on their own are less tolerant to mutation
353 and therefore more functionally important. This is supported by Muro et al. (38) who
354 recently found that genes which singly occupy a TAD are more likely to be associated with
355 disease. When we separated TADs into CTCF TADs and non CTCF TADs we found that this
356 relationship is stronger for CTCF TADs compared to non CTCF TADs (Supplementary figure
357 6). These results could indicate that there is a selective pressure for functionally important
358 genes to fall privately within CTCF TADs (formed by loop extrusion) providing them with
359 strong insulation from aberrant regulation. This selective pressure may be weaker for non
360 CTCF TADs which may not have been formed by loop extrusion and therefore may not be as
361 insulated. In contrast, we don't see this relationship at all for TopDom TADs, we propose
362 that this may be due to the smaller size of TopDom TADs which could reflect a scale more
363 similar to that of sub-TADs (10,39). It is also worth noting that TopDom annotates the entire
364 genome with TADs (compared to Arrowhead, which calls them sporadically) therefore if
365 regions exist in the genome which have no TADs, TopDom will still attempt to call them, this

366 could increase noise in TADs called by TopDom. The differences shown here between TADs
367 called using Arrowhead and TopDom highlight the importance of ensuring findings are
368 robust to the choice of TAD caller.

369 Our results indicate that there is little evidence for an increase in expression correlation or
370 functional annotation similarity in genes sharing a TAD. In general, we found no difference
371 in expression correlation between pairs of non-paralogous protein coding genes in CTCF
372 TADs vs random CTCF TADs. This is contrary to previous findings (16–19). We also found that
373 pairs of non-paralogous protein coding genes within CTCF TADs are largely not more similar
374 in functional annotation than in random TADs. This suggests that globally TADs are not
375 associated with a higher degree of co-regulation between the genes they contain.

376 Together our results suggest TADs play a stronger role in insulating genes from aberrant
377 regulation rather than promoting co-expression of genes within a TAD. We speculate that
378 our results are more compatible with a model of TADs in which enhancers are prevented
379 from interacting with all the genes within the same TAD by evolved enhancer-promoter
380 specificity or further insulation in the form of tissue/cell type specific sub-TADs. If this is the
381 case, disease associated variants within a TAD may have deleterious consequences by
382 misregulating their normal target gene, but also may acquire gain-of-function regulation of
383 other genes within the TAD.

384 Although referred to throughout as non CTCF TADs because they were identified by
385 published TAD callers these domains may not represent 'true' TADs based on the prevalent
386 definition (domains formed by loop extrusion). Instead, it is possible that these domains
387 represent other domain categories e.g. compartmental domains. We therefore suggest that
388 perhaps not all TADs called by TAD callers represent TADs. The results presented here

389 support the assertion made by Beagan et al. (10) that it is important to separate domains
390 formed by different mechanisms because they are likely to have different functional
391 properties.

392

393 CONCLUSIONS

394 Our results suggest a limited role for TADs in promoting co-regulation of the genes within
395 them. We find evidence that pairs of paralogous genes fall within TADs more often than
396 random TADs. However, we find that pairs of paralogous genes are only enriched in non
397 CTCF TADs. The functional differences observed between CTCF and non CTCF TADs may
398 reflect the possibility that non CTCF TADs are more similar to other types of chromatin
399 domain (e.g. compartmental domains) than TADs (defined loop extrusion). We find little
400 evidence that non-paralogous protein coding genes within the same CTCF TAD are more
401 likely to have correlated expression patterns or similar functional annotations than non-
402 paralogous protein coding genes in random TADs. This suggests that TADs formed by loop
403 extrusion do not have a global association with co-regulation and the formation of "gene
404 regulatory domains". We find evidence that genes that singly occupy a CTCF TAD have
405 significantly higher constraint. This suggests that these genes may be more functionally
406 important and TADs formed by loop extrusion may be acting to insulate them from aberrant
407 regulation. Overall, our results suggest a stronger role of TADs in regulatory insulation than
408 promotion of co-regulation.

409

410 METHODS

411 **Topologically associating domains**

412 Mouse ESC and Cortical neuron Hi-C data published in (24) was downloaded from Gene
413 Expression Omnibus (GEO) (accession number: GSE96107). These datasets represent two of
414 the high resolution mammalian Hi-C datasets published to date. Hi-C data was analysed
415 using the Juicer analysis pipeline aligning to the mm10 genome build (25). Parameters
416 within Juicer were selected so that contacts with a mapping quality (MAPQ) below 30 were
417 filtered. For each cell type all replicates were run through the Juicer pipeline separately and
418 were combined using the "mega" option in Juicer. Hi-C data was binned at 10kb and Vanilla
419 coverage (VC) normalisation was employed. The sex chromosomes where excluded from
420 analysis throughout.

421 It has been shown that algorithmically determined TADs can vary widely depending on the
422 TAD caller used (40–42). In order to make sure that results are robust to the choice of TAD
423 caller, TADs were called using Arrowhead and TopDom which were both run using default
424 parameters at 10kb. Arrowhead calls larger TADs, which can overlap whereas TopDom calls
425 smaller non-overlapping TADs. TADs were called on Hi-C maps made from merged
426 replicates.

427 It is widely suggested that TADs are formed by a loop extrusion process involving
428 convergent CTCF bound at TAD boundaries and cohesion (10). Where indicated, TADs have
429 been split into CTCF TAD or non CTCF TADs. In order to do this ESC and cortical neuron CTCF
430 ChIP-seq peaks (generated alongside the Hi-C data (24)) were downloaded from GEO (GEO
431 accession number: GSE96107). TADs where both boundaries were within ±1 bin (10kb) of a
432 CTCF peak were considered to be "CTCF TADs", the equivalent TADs in random TADs or
433 random genome TADs were used for comparison. Whereas, TADs with only one boundary or

434 neither boundary within ±1 bin (10kb) of a CTCF peak were considered to be “non CTCF
435 TADs”.

436

437 **Overlapping TADs with protein coding genes**

438 Ensembl IDs of mouse genes and mm10 coordinates were downloaded from BioMart (43)
439 and non-protein coding genes were filtered out. Using bedtools intersect (44), protein
440 coding genes were overlapped and assigned to a TAD if their start and end position fell
441 within the same TAD. This TAD-gene mapping method is more stringent than previously
442 used (16,17,38) but it allows us to focus on genes which can be confidently assigned to a
443 TAD and controls for the possibility that genes which overlap a TAD boundary may have
444 different features. This is especially important given recent evidence has shown that TAD
445 boundaries are often not “sharp”, instead boundaries can span “zones of transition”
446 meaning that it may not be possible to confidently assign genes spanning a TAD boundary to
447 one TAD or the other (45)

448 In order to assess the functional similarity between pairs of genes in TADs, where stated
449 olfactory genes were removed from analysis. The olfactory genes have undergone a
450 significant expansion in the mouse vs human genome. The human genome contains ~800
451 olfactory genes (of which <400 are functional), whereas the mouse genome contains ~1400
452 olfactory genes (of which <1050 are functional) (46). Therefore, in order to make the
453 findings of this study more relevant to human biology the olfactory genes were masked. To
454 achieve this MGI IDs associated with Olfactory genes were downloaded by identifying any
455 gene associated with the GO term: “olfactory receptor activity” (47–49) and IDs were

456 converted to ensembl IDs using BioMart, ensembl IDs were used to remove genes from the
457 analysis (1133 genes in total) (43).

458

459 **TAD randomisation and Genome randomisation**

460 We synthesised “random TADs” to serve as a null distributions to compare with TADs. To do
461 this we generated two TAD randomisation strategies, each controlling for a different
462 possible confounding signals. In the first strategy, which we refer to as “random TADs”, the
463 position of each TAD was randomised within the same chromosome so that each TAD was
464 randomly assigned to a new region of the same size as the original TAD. The new region was
465 accepted only if it contained the same number of genes as the original TAD. TopDom TADs
466 are non-overlapping, so overlapping was prohibited in random TopDom TADs. For each TAD,
467 if a new region satisfying the criteria could not be found after 10,000 attempts, the TAD was
468 excluded from the random TAD set. For TADs called using Arrowhead, we observed that the
469 overlap structure was far more likely to be “nested” (one TAD falls completely within
470 another) than “non-nested” (TADs overlap incompletely, with only part of the TAD falling
471 within the bounds of the other) (Supplementary figure 1). To approximate this overlap
472 structure in random TADs, every proposed new random TAD position was checked to see if
473 it overlapped any existing random TADs. If it overlapped an existing random TAD in a
474 “nested” fashion the overlap was always permitted. However, if it overlapped an existing
475 random TAD in a “non-nested” fashion, the new position was accepted with 10%
476 probability, thereby minimising this type of overlap. As with the random TopDom TADs, if a
477 position fulfilling this criteria could not be found after 10,000 attempts, the TAD was
478 excluded from the random TAD set. In the second randomisation method, which we refer to

479 as “random genome TADs” the position of TADs was maintained along with the number of
480 protein coding genes within them, but the order of the protein coding genes on each
481 chromosome was randomised. TAD randomisation methods were implemented using
482 pybedtools (50).

483 TADs called using Arrowhead and TopDom were randomised 100 times each, generating
484 100 sets each of: random Arrowhead TADs, random TopDom TADs, Arrowhead random
485 genome TADs and TopDom random genome TADs. Since, during the generation of each
486 random TAD set, the algorithm randomises the position of each TAD in turn, the order of
487 TADs was shuffled before the generation of every random TAD set. In order to test if 100
488 randomisation was enough, we plotted the median value of each measure investigated in
489 this study with each added random TAD/random genome TAD set. For most measures the
490 median begins to converge at fewer than 100 randomisations (Supplementary figure 8).

491 To test how our TAD randomisation algorithm performs compared to other recently
492 published methods we created TAD randomisation algorithms based on the descriptions in
493 Nora et al. 2012 (16) and Rao et al. 2014 (4). We used these algorithms to create example
494 random TAD sets and compared them to an example random TAD set created using our
495 method (Supplementary figure 1). In brief, in the Nora et al. 2012 method, each TAD was
496 randomised to a region on the same chromosome which contains the same number of
497 genes and is the same length or smaller than the original TAD. We adapted this method to
498 prevent overlapping when randomising TopDom TADs, if a non-overlapping TAD could not
499 be placed after 10,000 attempts it was excluded from the TopDom random TAD set. In the
500 Roa et al. 2014 method, each TAD was randomised to a new position on the same
501 chromosome but prevented from overlapping any gaps in the mm10 assembly (mm10 gaps

502 were downloaded from the UCSC table browser (51)). This method was adapted to prevent
503 overlapping when randomising TopDom TADs. Again, we set a cut off of 10,000 attempts to
504 place each TAD before it was excluded from the TopDom random TAD set.

505 We compared random TADs generated using our method to random TADs generated using
506 the Nora et al. 2012 method and the Roa et al. 2014 method (Supplementary figure 1). Since
507 the Nora el al. 2012 method does not generate any TADs containing zero genes, TADs with
508 zero genes were removed from all TAD sets before comparison. Regardless of the
509 randomisation method used, we observed that the distance between genes in random TADs
510 was always significantly different to the distance between genes in TADs. However, the
511 effect size of these differences was smallest for Arrowhead random TADs produced by our
512 method and second smallest for TopDom random TADs produced by our method (Rao et al.
513 2014 produces the smallest effect size for TopDom random TADs). This suggests that for this
514 feature, random TADs produced by our method are the closest of the three methods to real
515 Arrowhead TADs and second closest for TopDom TADs (Supplementary figure 1A).

516 We next compared the number of genes in random TADs. Again, TADs with zero genes were
517 removed before comparison. Since in our randomisation method and in the Nora et al. 2012
518 method, random TADs must contain the same number of genes as the original TADs, we did
519 not observe any difference between the number of genes within TADs and random TADs
520 using these methods. However, we did observe a significant difference (p-value<0.001)
521 between the number of genes in random TADs generated by the Rao et al. 2014 method
522 and TADs (except for TopDom ESC TADs which were not significantly different)
523 (Supplementary figure 1B). Therefore, random TADs produced using our method and the
524 Nora et al. 2012 method best reflect the number of genes in TADs.

525 The overlap structure of real Arrowhead TADs favours nested TADs. To assess how well each
526 randomisation method approximates the overlap structure of Arrowhead TADs, we selected
527 all TADs/random TADs which were involved in any type of overlap. We then annotated them
528 according to whether they were involved in nesting overlaps, non-nesting overlaps or both.
529 We found that our randomisation method best approximates the overlap structure of
530 Arrowhead TADs. Random Arrowhead TADs generated using the Rao et al. 2014 or the Nora
531 et al. 2012 method contain more non-nesting overlaps than Arrowhead TADs
532 (Supplementary figure 1C).

533

534 **Pairs of genes with shared ancestry:**

535 The functional similarity of genes within a TAD was measured by assessing the similarity of
536 every possible pair of genes within the same TAD. Gene pairs which have shared ancestry
537 i.e. paralogs, are expected to be very functionally similar. In order to assess whether genes
538 within TADs are more functional similar irrespective of shared ancestry, (where stated)
539 paralogous gene pairs were removed from the analysis. To do this mouse paralogous gene
540 pairs were downloaded from BioMart (Ensemble release 98) (43).

541

542 **Constraint score:**

543 Mouse gene constraint was assessed as a nonsynonymous z-score (32), calculated between
544 36 strains of mice commonly used for genetic research (52). In brief, constraint was
545 quantified for each gene as the deviation of the observed number of nonsynonymous
546 variants relative to the expected number given no selection, which was determined by the

547 average rate of synonymous fixation in the population sample. Genes that have a greater
548 relative depletion of nonsynonymous variants are considered more constrained by negative
549 selection.

550

551 **Functional enrichment analysis:**

552 Functional enrichment analysis was undertaken using the g:profiler r package (version
553 e100_eg47_p14_021df73) (53) and Biological processes GO terms. The plots include the
554 (max) top 25 most significant GO terms passing a p-value threshold of < 0.05 (multiple
555 testing corrected using the "gSCS" option). The similarity between each of the significant GO
556 terms was calculated using the r package GOSemSim (54) (using the "Jiang" similarity
557 method as the "measure" parameter and "NULL" as the "combine" parameter). These
558 similarity scores were then used as input into hclust clustering, the order resulting from
559 clustering was used to order the GO terms in the plots.

560

561 **Gene co-expression:**

562 FPKM counts from RNA-seq data generated alongside the Hi-C data was downloaded from
563 GEO (GEO accession number: GSE96107). The data consisted of two replicates each for ESC,
564 neural progenitor cells (NPC), and cortical neurons. Genes with an FPKM value <1 were
565 treated as having 0 expression. Gene co-expression was calculated across all 6 samples using
566 spearman's rank correlation coefficient between all pairs of genes. Correlation coefficients
567 calculated from this data indicate the similarity of expression over three cell types.

568 To guard against the possibility that TAD structure may differ between cell types we also
569 downloaded RNA seq data from the closest matching tissues/cell types to ESCs and cortical
570 neurons which had at least 3 samples (required for the correlation analyses) from the
571 Encode project (33) and GEO (35). To assess the expression correlation within cortical
572 neuron TADs we downloaded encode forebrain RNA-seq. The forebrain RNA-seq was
573 generated with two replicates each, of embryos of varying ages. Accession numbers:
574 ENCFF302TQO, ENCFF976OLT, ENCFF895JXR, ENCFF227HKF, ENCFF340XFQ, ENCFF484AOO,
575 ENCFF601JPN, ENCFF413BXV, ENCFF465SNB, ENCFF567AFL, ENCFF590FAC, ENCFF745ZJF,
576 ENCFF763GXJ, ENCFF804FTJ, ENCFF816CVP and ENCFF918QNL (33,34). Genes with an FPKM
577 value <1 were treated as having 0 expression. To assess the expression correlation within
578 ESC TADs we downloaded mouse ESCs differentiating to PGC RNA-seq data. The ESCs
579 differentiating to PGC RNA-seq data was generated with three replicates each of ESC,
580 epiblast like cells (day 2), PGC (day 4) and PGC (day 6) (36). Processed RNA-seq data was
581 downloaded from GEO accession GSE86903, data was provided as $\log_2$(RPM) which we
582 converted to RPKM for analysis. Genes with an RPKM value <1 were treated as having 0
583 expression.

584

585 **GO Semantic similarity:**

586 The R package GOSemSim (54) was used to calculate GO semantic similarity scores. For each
587 pair of genes the GO terms assigned to them were compared using the Jiang method. If
588 genes were associated with multiple GO terms, scores were combined using “best match
589 average”. Pairs of genes where one or both have no annotated GO terms were excluded
590 from the analysis as no score could be generated. We first calculated the similarity score

591 between all pairs of genes in the genome using each of the MF, Biological process (BP) or
592 Cellular component (CC) ontologies. We then plotted these scores for all autosomal genes,
593 autosomal genes minus olfactory genes, and autosomal genes minus olfactory genes and
594 paralogous pairs, against genomic distance in the real genome compared to the median
595 distance in 1000 random genomes. We found that, for scores calculated with BP and CC,
596 once olfactory genes and paralogous gene pairs have been removed there is no association
597 between GO similarity and distance. This suggests that similarity in these scores is driven by
598 paralogous pairs and the olfactory genes. We therefore moved forward using only MF in our
599 analysis (Supplementary figure 9).

600

601 **Shared pathways**

602 Kegg pathways were downloaded from org.Mm.eg.db (55). The Kegg pathway data is very
603 sparse and many genes do not have a pathway annotation. In order to account for this, the
604 amount of pairs of genes sharing at least one pathway annotation was considered as a
605 proportion of all pairs of genes with at least one pathway annotation each.

606

607 **Shared protein-protein interactions (PPIs)**

608 PPI data was downloaded for mm10 from string v11 (56). Only interactions with the mode
609 "binding" were selected so that only direct/physical interactions (rather than functional
610 interactions which may not require physical contact) were included. Similarly to pathways,
611 PPI data is very sparse and many genes are unannotated. Therefore, as with pathways the

612 amount of pairs of genes with a PPI was considered as a proportion of all pairs of genes with
613 at least one PPI annotation each.

614

615 **Random permutation testing**

616 For expression correlation, GO semantic similarity, proportion of gene pairs sharing a
617 pathway and proportion of genes pairs sharing a PPI we have plotted the functional score
618 against binned genomic distance in the real genome and compared it to the median value of
619 the functional score in 1000 random genomes. In these analyses for each bin, we have
620 established whether there is a significant difference between the functional score in the real
621 genome compared to the distribution of scores in 1000 random genomes using permutation
622 testing. For each bin this has been calculated as follows: sum(values in the random genome
623 ≥ value in the real genome)/1000. P-values were then FDR corrected.

624

625 **Effect size**

626 Effect size, r, was calculated using the r package rcompanion. A positive effect size indicates
627 that the value associated with TADs is greater (than random TADs/random genome TADs)
628 whereas a negative effect size indicates that the value associated with TADs is lesser (than
629 random TADs/random genome TADs). The larger the value the larger the effect size.

630

631 ## LIST OF ABBREVIATIONS

632 CN- Cortical neurons

633 ESC- Embryonic stem cells

634 FPKM- Fragments Per Kilobase of transcript per Million mapped reads

635 GEO- Gene Expression Omnibus

636 GO- Gene ontology

637 MAPQ- MAPping Quality

638 MF- Molecular function

639 NPC- Neural progenitor cells

640 NS- Not significant

641 PGC- Primordial germ cell

642 PPI- Protein- protein interactions

643 RPKM- Reads Per Kilobase of transcript per Million mapped reads

644 TAD- Topologically associating domains

645

646 AVAILABILITY OF DATA AND MATERIALS

647 The processed datasets analysed in the current study will be made available upon

648 publication.

649

650 REFERENCES

651 1. Rowley MJ, Corces VG. Organizational principles of 3D genome architecture. Nat Rev Genet

652 [Internet]. 2018 Dec 26 [cited 2019 Oct 28];19(12):789–800. Available from:

653 http://www.nature.com/articles/s41576-018-0060-8

654 2. Dekker J, Rippe K, Dekker M, Kleckner N. Capturing chromosome conformation. Science
655 [Internet]. 2002 Feb 15 [cited 2018 Nov 23];295(5558):1306–11. Available from:
656 http://www.ncbi.nlm.nih.gov/pubmed/11847345

657 3. Lieberman-Aiden E, van Berkum NL, Williams L, Imakaev M, Ragoczy T, Telling A, et al.
658 Comprehensive mapping of long-range interactions reveals folding principles of the human
659 genome. Science [Internet]. 2009 Oct 9 [cited 2018 Feb 28];326(5950):289–93. Available
660 from: http://www.ncbi.nlm.nih.gov/pubmed/19815776

661 4. Rao SSP, Huntley MH, Durand NC, Stamenova EK, Bochkov ID, Robinson JT, et al. A 3D map of
662 the human genome at kilobase resolution reveals principles of chromatin looping. Cell
663 [Internet]. 2014 Dec 18 [cited 2018 Aug 13];159(7):1665–80. Available from:
664 http://www.ncbi.nlm.nih.gov/pubmed/25497547

665 5. Hildebrand EM, Dekker J. Mechanisms and Functions of Chromosome Compartmentalization.
666 Vol. 45, Trends in Biochemical Sciences. Elsevier Ltd; 2020. p. 385–96.

667 6. Dixon JR, Selvaraj S, Yue F, Kim A, Li Y, Shen Y, et al. Topological domains in mammalian
668 genomes identified by analysis of chromatin interactions. Nature [Internet]. 2012 Apr 11
669 [cited 2018 Feb 5];485(7398):376–80. Available from:
670 http://www.nature.com/doifinder/10.1038/nature11082

671 7. Nuebler J, Fudenberg G, Imakaev M, Abdennur N, Mirny LA. Chromatin organization by an
672 interplay of loop extrusion and compartmental segregation. Proc Natl Acad Sci U S A. 2018 Jul
673 17;115(29):E6697–706.

674 8. Mirny LA, Imakaev M, Abdennur N. Two major mechanisms of chromosome organization.
675 Curr Opin Cell Biol [Internet]. 2019 Jun 19 [cited 2019 Jul 8];58:142–52. Available from:
676 http://www.ncbi.nlm.nih.gov/pubmed/31228682

677 9. Schmitt AD, Hu M, Jung I, Xu Z, Qiu Y, Tan CL, et al. A Compendium of Chromatin Contact
678 Maps Reveals Spatially Active Regions in the Human Genome. Cell Rep [Internet]. 2016 Nov
679 15 [cited 2018 May 16];17(8):2042–59. Available from:
680 https://www.sciencedirect.com/science/article/pii/S2211124716314814?via%3Dihub#mmc1

681 10. Beagan JA, Phillips-Cremins JE. On the existence and functionality of topologically associating
682 domains. Nat Genet [Internet]. 2020 Jan 10 [cited 2020 Jan 13]; Available from:
683 http://www.nature.com/articles/s41588-019-0561-1

684 11. Dixon JR, Gorkin DU, Ren B. Chromatin Domains: The Unit of Chromosome Organization. Mol
685 Cell [Internet]. 2016 [cited 2018 Apr 16];62:668–80. Available from:
686 http://dx.doi.org/10.1016/j.molcel.2016.05.018

687 12. Symmons O, Uslu VV, Tsujimura T, Ruf S, Nassari S, Schwarzer W, et al. Functional and
688 topological characteristics of mammalian regulatory domains. Genome Res [Internet]. 2014
689 Mar [cited 2018 Feb 5];24(3):390–400. Available from:
690 http://www.ncbi.nlm.nih.gov/pubmed/24398455

691 13. Franke M, Ibrahim DM, Andrey G, Schwarzer W, Heinrich V, Schöpflin R, et al. Formation of
692 new chromatin domains determines pathogenicity of genomic duplications. Nature
693 [Internet]. 2016 Oct 5 [cited 2018 Mar 7];538(7624):265–9. Available from:
694 http://www.nature.com/articles/nature19800

695 14. Scacheri CA, Scacheri PC. Mutations in the noncoding genome. Curr Opin Pediatr [Internet].
696 2015 Dec [cited 2018 Mar 8];27(6):659–64. Available from:
697 http://www.ncbi.nlm.nih.gov/pubmed/26382709

698 15. Dixon JR, Jung I, Selvaraj S, Shen Y, Antosiewicz-Bourget JE, Lee AY, et al. Chromatin
699 architecture reorganization during stem cell differentiation. Nature [Internet]. 2015 Feb 19
700 [cited 2018 Nov 22];518(7539):331–6. Available from:

701 http://www.ncbi.nlm.nih.gov/pubmed/25693564

702 16. Nora EP, Lajoie BR, Schulz EG, Giorgetti L, Okamoto I, Servant N, et al. Spatial partitioning of
703 the regulatory landscape of the X-inactivation centre. Nature [Internet]. 2012 Apr 11 [cited
704 2018 Nov 23];485(7398):381–5. Available from:
705 http://www.nature.com/doifinder/10.1038/nature11049

706 17. Flavahan WA, Drier Y, Liau BB, Gillespie SM, Venteicher AS, Stemmer-Rachamimov AO, et al.
707 Insulator dysfunction and oncogene activation in IDH mutant gliomas. Nature. 2016 Jan
708 7;529(7584):110–4.

709 18. Tarbier M, Mackowiak SD, Frade J, Catuara-Solarz S, Biryukova I, Gelali E, et al. Nuclear gene
710 proximity and protein interactions shape transcript covariances in mammalian single cells.
711 bioRxiv. 2019 Sep 16;771402.

712 19. Sarnataro S, Riba A, Molina N. Regulation of transcription reactivation dynamics exiting
713 mitosis. bioRxiv. 2020 Apr 16;2020.04.15.042853.

714 20. Ruiz-Velasco M, Zaugg JB. Structure meets function: How chromatin organisation conveys
715 functionality. Curr Opin Syst Biol [Internet]. 2017 Feb 1 [cited 2019 Jan 10];1:129–36.
716 Available from:
717 https://www.sciencedirect.com/science/article/pii/S2452310017300173?dgcid=raven_sd_re
718 commender_email

719 21. Neems DS, Garza-Gongora AG, Smith ED, Kosak ST. Topologically associated domains
720 enriched for lineage-specific genes reveal expression-dependent nuclear topologies during
721 myogenesis. Proc Natl Acad Sci [Internet]. 2016 Mar 22 [cited 2019 Jan 10];113(12):E1691–
722 700. Available from: https://www.pnas.org/content/113/12/E1691.long

723 22. Hurst LD, Pál C, Lercher MJ. The evolutionary dynamics of eukaryotic gene order. Nat Rev
724 Genet [Internet]. 2004 Apr [cited 2019 Aug 23];5(4):299–310. Available from:

725 http://www.nature.com/articles/nrg1319

726 23. Thévenin A, Ein-Dor L, Ozery-Flato M, Shamir R. Functional gene groups are concentrated
727 within chromosomes, among chromosomes and in the nuclear space of the human genome.
728 Nucleic Acids Res [Internet]. 2014 Sep 2 [cited 2019 Apr 24];42(15):9854–61. Available from:
729 http://academic.oup.com/nar/article/42/15/9854/2435256/Functional-gene-groups-are-
730 concentrated-within

731 24. Bonev B, Mendelson Cohen N, Szabo Q, Fritsch L, Papadopoulos GL, Lubling Y, et al.
732 Multiscale 3D Genome Rewiring during Mouse Neural Development. Cell [Internet]. 2017 Oct
733 19 [cited 2018 Dec 7];171(3):557-572.e24. Available from:
734 http://www.ncbi.nlm.nih.gov/pubmed/29053968

735 25. Durand NC, Shamim MS, Machol I, Rao SSP, Huntley MH, Lander ES, et al. Juicer Provides a
736 One-Click System for Analyzing Loop-Resolution Hi-C Experiments. Cell Syst [Internet]. 2016
737 Jul 27 [cited 2018 Jul 30];3(1):95–8. Available from:
738 https://www.sciencedirect.com/science/article/pii/S2405471216302198?via%3Dihub

739 26. Shin H, Shi Y, Dai C, Tjong H, Gong K, Alber F, et al. TopDom: an efficient and deterministic
740 method for identifying topological domains in genomes. Nucleic Acids Res [Internet]. 2016
741 Apr 20 [cited 2018 Jun 21];44(7):e70–e70. Available from:
742 https://academic.oup.com/nar/article-lookup/doi/10.1093/nar/gkv1505

743 27. Sanborn AL, Rao SSP, Huang S-C, Durand NC, Huntley MH, Jewett AI, et al. Chromatin
744 extrusion explains key features of loop and domain formation in wild-type and engineered
745 genomes. Proc Natl Acad Sci U S A [Internet]. 2015 Nov 24 [cited 2018 Nov
746 28];112(47):E6456-65. Available from: http://www.ncbi.nlm.nih.gov/pubmed/26499245

747 28. Vietri Rudan M, Barrington C, Henderson S, Ernst C, Odom DT, Tanay A, et al. Comparative Hi-
748 C reveals that CTCF underlies evolution of chromosomal domain architecture. Cell Rep

749 [Internet]. 2015 Mar 3 [cited 2019 Jan 9];10(8):1297–309. Available from:
750 http://www.ncbi.nlm.nih.gov/pubmed/25732821

751 29. Stamboulian M, Guerrero RF, Hahn MW, Radivojac P. The ortholog conjecture revisited: The
752 value of orthologs and paralogs in function prediction. Bioinformatics [Internet]. 2020 [cited
753 2021 Apr 13];36(Suppl 1):I219–26. Available from: /pmc/articles/PMC7355290/

754 30. Ibn-Salem J, Muro EM, Andrade-Navarro MA. Co-regulation of paralog genes in the three-
755 dimensional chromatin architecture. Nucleic Acids Res. 2017;45(1):81–91.

756 31. Bartha I, Di Iulio J, Venter JC, Telenti A. Human gene essentiality. Nat Rev Genet [Internet].
757 2018 Oct 30 [cited 2020 Sep 24];19(1):51–62. Available from: www.nature.com/nrg

758 32. Powell G, Simon M, Pulit S, Mallon A-M, Lindgren C. Tolerance of nonsynonymous variation is
759 closely correlated between human and mouse orthologues. bioRxiv [Internet]. 2019 Jun 3
760 [cited 2020 Sep 24];657981. Available from: https://doi.org/10.1101/657981

761 33. Davis CA, Hitz BC, Sloan CA, Chan ET, Davidson JM, Gabdank I, et al. The Encyclopedia of DNA
762 elements (ENCODE): Data portal update. Nucleic Acids Res [Internet]. 2018 Jan 1 [cited 2020
763 Sep 25];46(D1):D794–801. Available from: https://pubmed.ncbi.nlm.nih.gov/29126249/

764 34. He P, Williams BA, Trout D, Marinov GK, Amrhein H, Berghella L, et al. The changing mouse
765 embryo transcriptome at whole tissue and single-cell resolution. Nature. 2020 Jul
766 30;583(7818):760–7.

767 35. Edgar R, Domrachev M, Lash AE. Gene Expression Omnibus: NCBI gene expression and
768 hybridization array data repository. Nucleic Acids Res [Internet]. 2002 Jan 1 [cited 2018 Nov
769 19];30(1):207–10. Available from: http://www.ncbi.nlm.nih.gov/pubmed/11752295

770 36. von Meyenn F, Berrens R V., Andrews S, Santos F, Collier AJ, Krueger F, et al. Comparative
771 Principles of DNA Methylation Reprogramming during Human and Mouse In Vitro Primordial
772 Germ Cell Specification. Dev Cell [Internet]. 2016 Oct 10 [cited 2021 Apr 7];39(1):104–15.

773 Available from: https://pubmed.ncbi.nlm.nih.gov/27728778/

774 37. Soler-Oliva ME, Guerrero-Martínez JA, Bachetti V, Reyes JC. Analysis of the relationship
775 between coexpression domains and chromatin 3D organization. PLoS Comput Biol. 2017 Sep
776 1;13(9).

777 38. Muro EM, Ibn-Salem J, Andrade-Navarro MA. The distributions of protein coding genes within
778 chromatin domains in relation to human disease. Epigenetics and Chromatin [Internet]. 2019
779 Dec 5 [cited 2020 Mar 10];12(1):72. Available from:
780 https://epigeneticsandchromatin.biomedcentral.com/articles/10.1186/s13072-019-0317-2

781 39. Phillips-Cremins JE, Sauria MEG, Sanyal A, Gerasimova TI, Lajoie BR, Bell JSK, et al.
782 Architectural Protein Subclasses Shape 3D Organization of Genomes during Lineage
783 Commitment. Cell [Internet]. 2013 Jun 6 [cited 2018 Feb 5];153(6):1281–95. Available from:
784 http://www.ncbi.nlm.nih.gov/pubmed/23706625

785 40. Dali R, Blanchette M. A critical assessment of topologically associating domain prediction
786 tools. Nucleic Acids Res [Internet]. 2017 Apr 7 [cited 2018 May 4];45(6):2994–3005. Available
787 from: https://academic.oup.com/nar/article-lookup/doi/10.1093/nar/gkx145

788 41. Forcato M, Nicoletti C, Pal K, Livi CM, Ferrari F, Bicciato S. Comparison of computational
789 methods for Hi-C data analysis. Nat Methods. 2017;14(7).

790 42. Zufferey M, Tavernari D, Oricchio E, Ciriello G. Comparison of computational methods for the
791 identification of topologically associating domains. Genome Biol [Internet]. 2018 Dec 10
792 [cited 2018 Dec 12];19(1):217. Available from:
793 https://genomebiology.biomedcentral.com/articles/10.1186/s13059-018-1596-9

794 43. Smedley D, Haider S, Ballester B, Holland R, London D, Thorisson G, et al. BioMart - Biological
795 queries made easy. BMC Genomics [Internet]. 2009 Jan 14 [cited 2020 Mar 10];10(1):22.
796 Available from: http://bmcgenomics.biomedcentral.com/articles/10.1186/1471-2164-10-22

797 44. Quinlan AR, Hall IM. BEDTools: A flexible suite of utilities for comparing genomic features.
798 Bioinformatics [Internet]. 2010 Jan 28 [cited 2020 Sep 25];26(6):841–2. Available from:
799 /pmc/articles/PMC2832824/?report=abstract

800 45. Chang LH, Ghosh S, Noordermeer D. TADs and Their Borders: Free Movement or Building a
801 Wall? Vol. 432, Journal of Molecular Biology. Academic Press; 2020. p. 643–52.

802 46. Niimura Y. Evolutionary dynamics of olfactory receptor genes in chordates: interaction
803 between environments and genomic contents. Vol. 4, Human genomics. BioMed Central;
804 2009. p. 107–18.

805 47. Carbon S, Ireland A, Mungall CJ, Shu S, Marshall B, Lewis S, et al. AmiGO: online access to
806 ontology and annotation data. Bioinforma Appl NOTE [Internet]. 2009 [cited 2020 Mar
807 10];25(2):288–9. Available from: http://www.geneontology.org

808 48. The Gene Ontology Consortium. The Gene Ontology Resource: 20 years and still GOing
809 strong. Nucleic Acids Res [Internet]. 2018 Nov 5;47(D1):D330–8. Available from:
810 https://doi.org/10.1093/nar/gky1055

811 49. Ashburner M, Ball CA, Blake JA, Botstein D, Butler H, Cherry JM, et al. Gene ontology: Tool for
812 the unification of biology. Vol. 25, Nature Genetics. NIH Public Access; 2000. p. 25–9.

813 50. Dale RK, Pedersen BS, Quinlan AR. Pybedtools: A flexible Python library for manipulating
814 genomic datasets and annotations. Bioinformatics [Internet]. 2011 Dec [cited 2020 Sep
815 25];27(24):3423–4. Available from: https://pubmed.ncbi.nlm.nih.gov/21949271/

816 51. Karolchik D, Hinricks AS, Furey TS, Roskin KM, Sugnet CW, Haussler D, et al. The UCSC table
817 browser data retrieval tool. Nucleic Acids Res [Internet]. 2004 Jan 1 [cited 2020 Sep
818 25];32(DATABASE ISS.). Available from: https://pubmed.ncbi.nlm.nih.gov/14681465/

819 52. Keane TM, Goodstadt L, Danecek P, White MA, Wong K, Yalcin B, et al. Mouse genomic
820 variation and its effect on phenotypes and gene regulation. Nature [Internet]. 2011 Sep 15

821 [cited 2018 Dec 11];477(7364):289–94. Available from:
822 http://www.nature.com/articles/nature10413

823 53. Raudvere U, Kolberg L, Kuzmin I, Arak T, Adler P, Peterson H, et al. g:Profiler: a web server for
824 functional enrichment analysis and conversions of gene lists (2019 update). Nucleic Acids Res
825 [Internet]. 2019 May 8;47(W1):W191–8. Available from: https://doi.org/10.1093/nar/gkz369

826 54. Yu G, Li F, Qin Y, Bo X, Wu Y, Wang S. GOSemSim: an R package for measuring semantic
827 similarity among GO terms and gene products. Bioinformatics [Internet]. 2010 Apr 1 [cited
828 2019 Jul 17];26(7):976–8. Available from: https://academic.oup.com/bioinformatics/article-
829 lookup/doi/10.1093/bioinformatics/btq064

830 55. Carlson M. org.Mm.eg.db: Genome wide annotation for Mouse. R package version 3.5.0.
831 Bioconductor. 2017.

832 56. Szklarczyk D, Gable AL, Lyon D, Junge A, Wyder S, Huerta-Cepas J, et al. STRING v11: Protein-
833 protein association networks with increased coverage, supporting functional discovery in
834 genome-wide experimental datasets. Nucleic Acids Res. 2019 Jan 8;47(D1):D607–13.

835

836 # DECLARATIONS

837 ## Ethics approval and consent to participate

838 Not applicable.

839 ## Consent for publication

840 Not applicable.

841 ## Competing interests

842 The authors declare they have no competing financial interests.

Funding

Research reported in this publication was supported by the Medical Research Council (MC_U142684171) and National Human Genome Research Institute of the National Institutes of health (UM1HG006370). The content is solely the responsibility of the authors and does not necessarily represent the official views of the National Institutes of Health.

The research was also supported by the Wellcome Trust Core Award Grant Number 203141/Z/16/Z with additional support from the NIHR Oxford BRC. The views expressed are those of the authors and not necessarily those of the NHS, the NIHR or the Department of Health.

Authors' contributions

HSL and MMS conceived and directed the research. HSL carried out the majority of the analysis and wrote the manuscript. SG provided statistical insight. GP calculated the constraint scores. AMM, CML and MMS provided critical feedback and supervised this work. All authors approved the manuscript.

Acknowledgements

We would like to acknowledge the helpful feedback and comments given by Dr Christoffer Nellåker and Dr Saskia Reibe during the preparation of this manuscript.

Authors' information (optional)

Footnotes

FIGURES

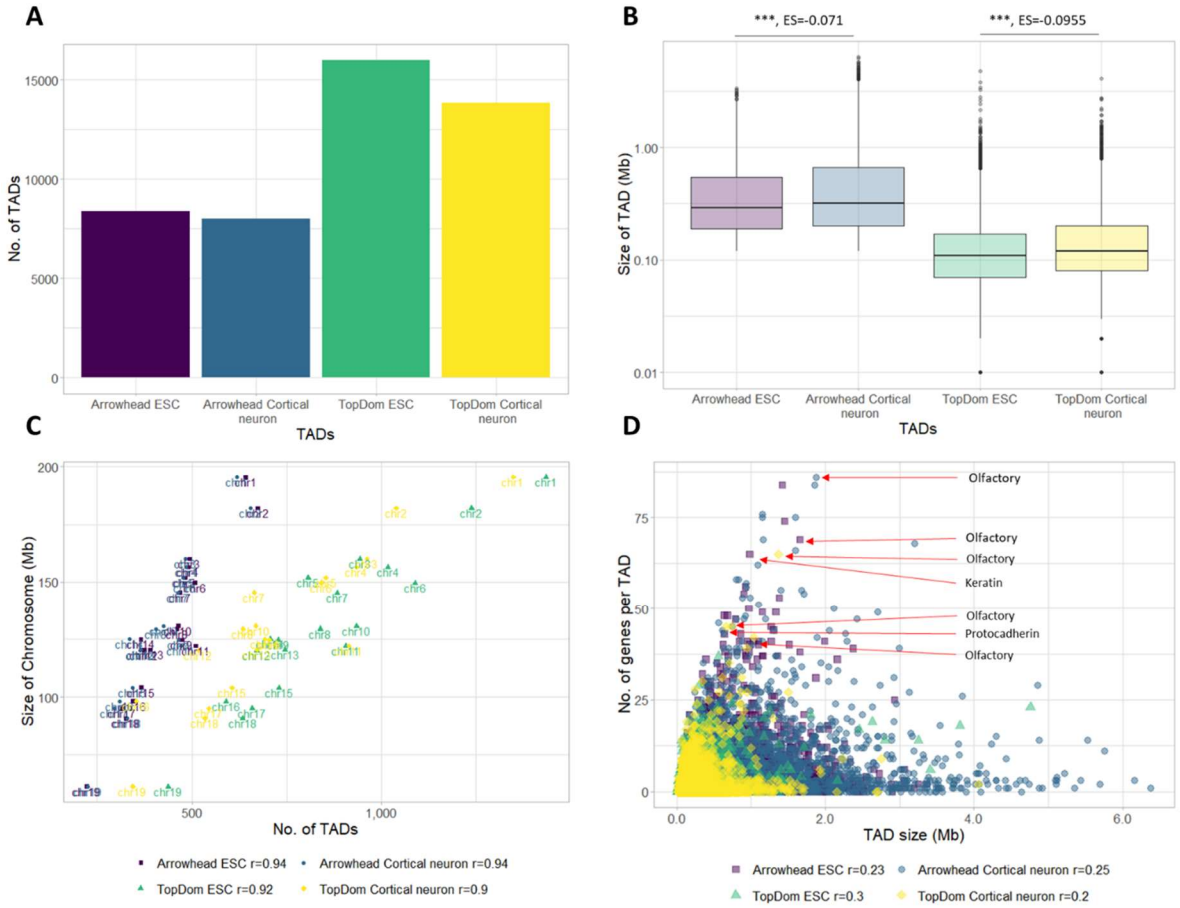

Figure 1: Features of autosomal TADs in ESCs and cortical neurons. *A) The number of TADs called using Arrowhead and TopDom in ESCs and cortical neurons. Arrowhead calls fewer TADs than TopDom in both cell types. More TADs are called in ESCs than cortical neurons with both TAD callers. B) Size of TADs called using Arrowhead and TopDom in ESCs and cortical neurons (plotted on a log10 scale). Arrowhead calls larger TADs than TopDom in both cell types. Both Arrowhead and TopDom call significantly smaller TADs in ESCs than cortical neurons (Wilcoxon test, p-value: p<0.001 = ***, p<0.01 = **, p<0.05 = *, ES= Effect size calculated using r for Wilcoxon). C) The number of TADs per chromosome is strongly correlated with the size of the chromosome. D) In both cell types and with both TAD callers most TADs have few genes. Overall, there is a low correlation between TAD size and gene number. Several TADs containing many genes were further investigated and found to contain multiple members of large gene families (annotated).*

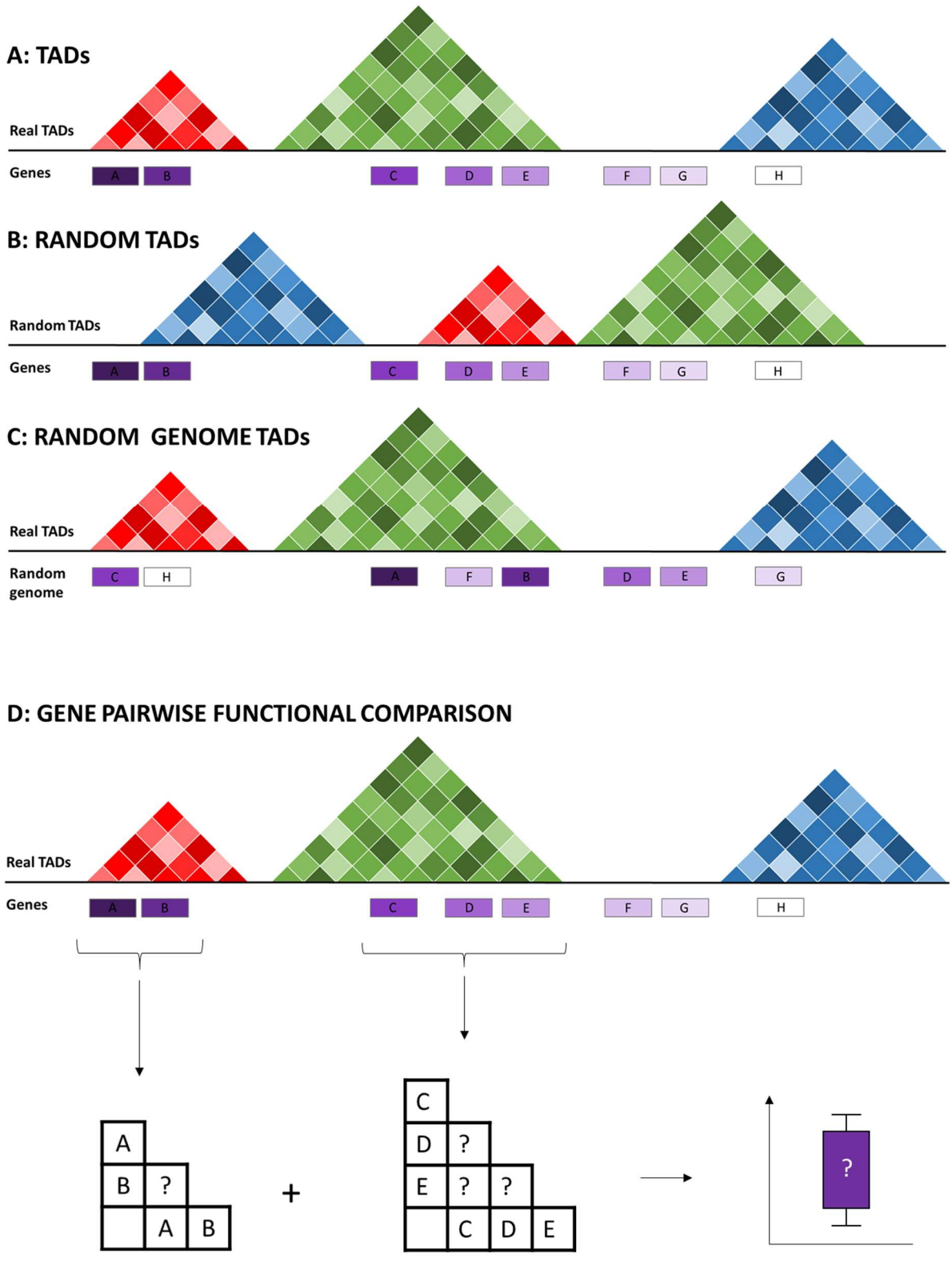

Figure 2: Randomization and functional analysis procedure. *A: Schematic representing the structure of annotated TADs. B: Null dataset one: Random TADs. TADs were randomised within the*

880 *same chromosome by selecting regions of equal size to the original TAD which also contain the same*

881 *number of genes, thus controlling for the effect of the linear genome. C: Null dataset two: Random*

882 *genome TADs. In order to remove the effect of the linear genome another null TAD set was*

883 *generated in which the TADs remained in the same positions but the order of genes on the*

884 *chromosome were randomised. C: Pairwise strategy for comparing functional similarity between*

885 *genes in the same TAD. All possible pairs of genes in each TAD were compared.*

886

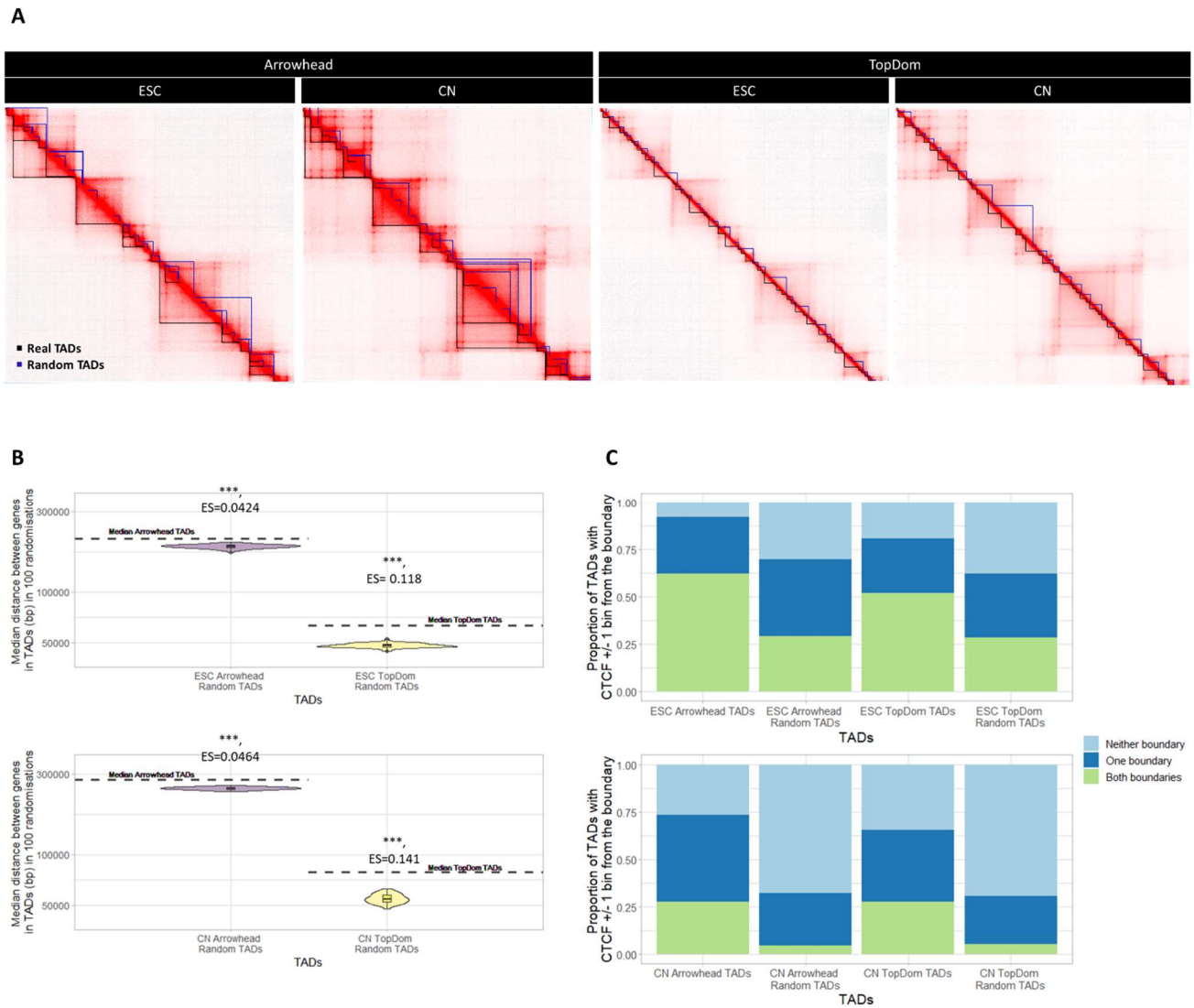

887

888 ***Figure 3: Features of autosomal TADs vs random TADs.*** *A) TADs (black) vs an example set of random*

889 *TADs (blue) shown on the Hi-C matrix for the equivalent region of Chr2 in both ESCs and cortical*

890 *neurons (CN). Matrices visualised using JuiceBox. B) Median distance between genes in TADs (dotted*
891 *line) vs the median distance between genes in 100 sets of random TADs (plotted on a log10 scale).*
892 *Genes are significantly closer together in random TADs than TADs (Wilcoxon test, Median p-value:*
893 *p<0.001 = ***, p<0.01 = **, p<0.05 = *, ES= Median effect size calculated using r for Wilcoxon). C)*
894 *Proportion of TADs with a CTCF binding site within ±10kb of both boundaries, one boundary or*
895 *neither boundary. As expected a greater proportion of TADs have a CTCF binding site near both*
896 *boundaries than in an example set of random TADs.*

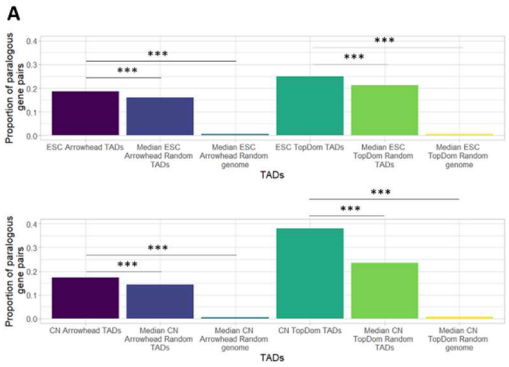

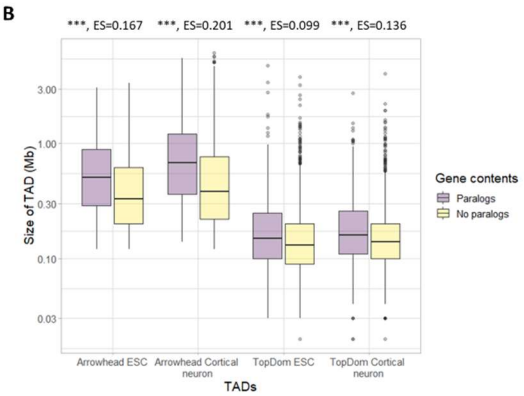

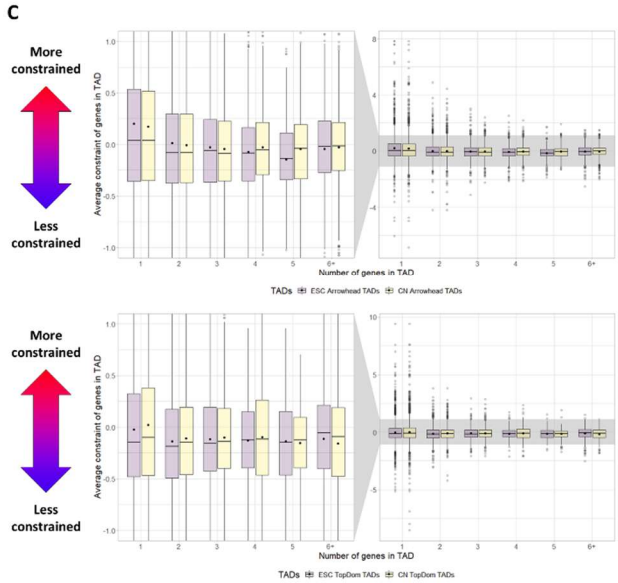

D

Wilcoxon Rank Sum between average gene constraint in TADs containing 1, 2, 3, 4, 5, 6+ genes					
No. of genes in TAD	No. of genes in TAD	ESC Arrowhead TADs p-value	CN Arrowhead TADs p-value	ESC TopDom TADs p-value	CN TopDom TADs p-value
1	2	7.02891E-05	4.80922E-05	0.05682289	0.03668281
1	3	6.25276E-05	4.29865E-05	0.60674695	0.2885912
1	4	6.25276E-05	0.006711671	0.78545567	0.72993771
1	5	2.36841E-06	0.002484544	0.60674695	0.37532039
1	6+	7.02891E-05	0.000387902	0.78545567	0.2885912
2	3	0.604083544	0.653850845	0.49899563	0.88222468
2	4	0.361851824	0.608252477	0.51958783	0.88222468
2	5	0.020258286	0.842273353	0.78545567	0.91952944
2	6+	0.518659548	0.162276223	0.07477507	0.94735077
3	4	0.557301168	0.385518081	0.87715304	0.88222468
3	5	0.061758268	0.842273353	0.8078207	0.88222468
3	6+	0.312254491	0.045194439	0.49899563	0.94735077
4	5	0.180949969	0.608252477	0.8078207	0.88222468
4	6+	0.079572481	0.608252477	0.49899563	0.88222468
5	6+	0.001207233	0.23216969	0.49899563	0.88222468

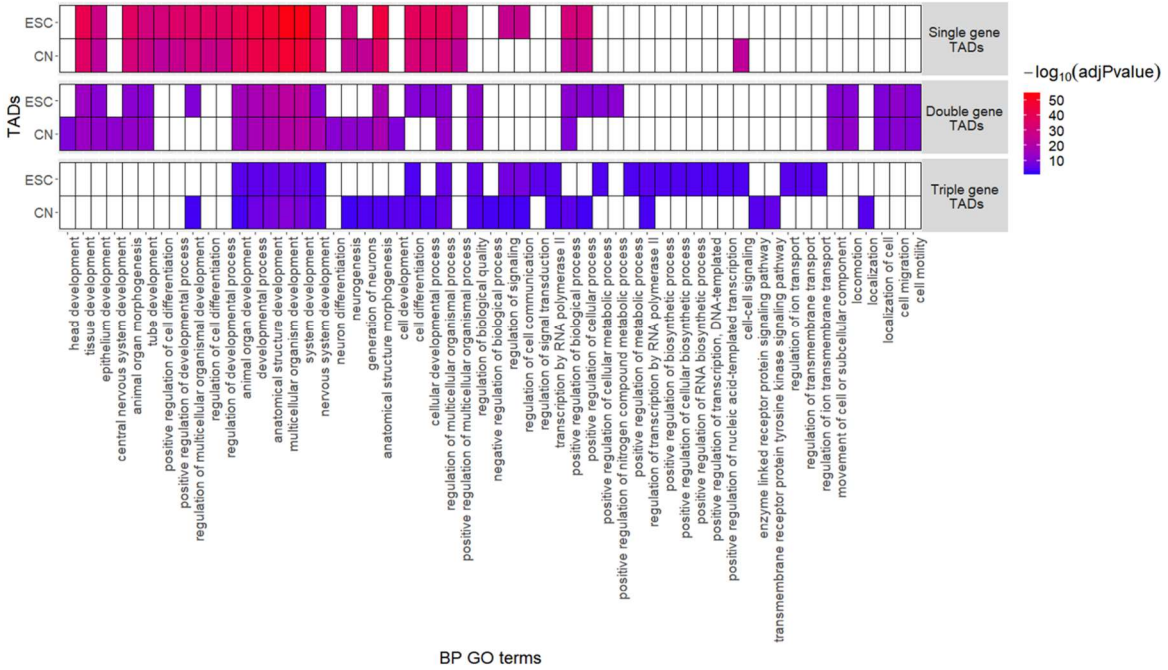

897

898 ***Figure 4: Paralogs and constraint vs autosomal TADs.*** *A) Proportion of paralogous gene pairs in*
899 *TADs, the median proportion in 100 sets of random TADs, and the median proportion in 100 sets of*
900 *random genome TADs. TADs contain significantly more pairs of paralogous genes than both random*
901 *TADs and random genome TADs (Fisher's exact test, Median p-value: p<0.001 = ***, p<0.01 = **,*
902 *p<0.05 = *). B) Size of TADs containing pairs of paralogs vs TADs (with >1 gene) containing no pairs of*
903 *paralogs (plotted on a log10 scale). For both TAD callers and cell types, TADs which contain pairs of*
904 *paralogs are larger than TADs which have no paralog pairs. (Wilcoxon test, p-value: p<0.001 = ***,*
905 *p<0.01 = **, p<0.05 = *, ES= Effect size calculated using r for Wilcoxon). C) Distribution of mean*
906 *constraint scores of genes occupying the same TAD. TADs are split depending on the number of genes*
907 *they contain (1, 2, 3, 4, 5, 6+). Dots indicate the mean of the distribution. D) Table showing FDR*
908 *corrected p-values of differences between groups in C calculated with the Wilcoxon test. Significant*
909 *p-values are highlighted red. For TADs called using Arrowhead in both cell types, genes singly*
910 *occupying a TAD have a significantly higher constraint score than the average constraint of genes in*
911 *TADs with >1 gene. For TADs called using TopDom no significant difference is observed. E) Biological*
912 *processes GO term functional enrichment of genes singly, doubly or triply occupying an Arrowhead*
913 *TAD. Only the top 25 most significant GO terms passing a p-value threshold of < 0.05 (multiple*
914 *testing corrected using the "gSCS" option) are shown.*

915

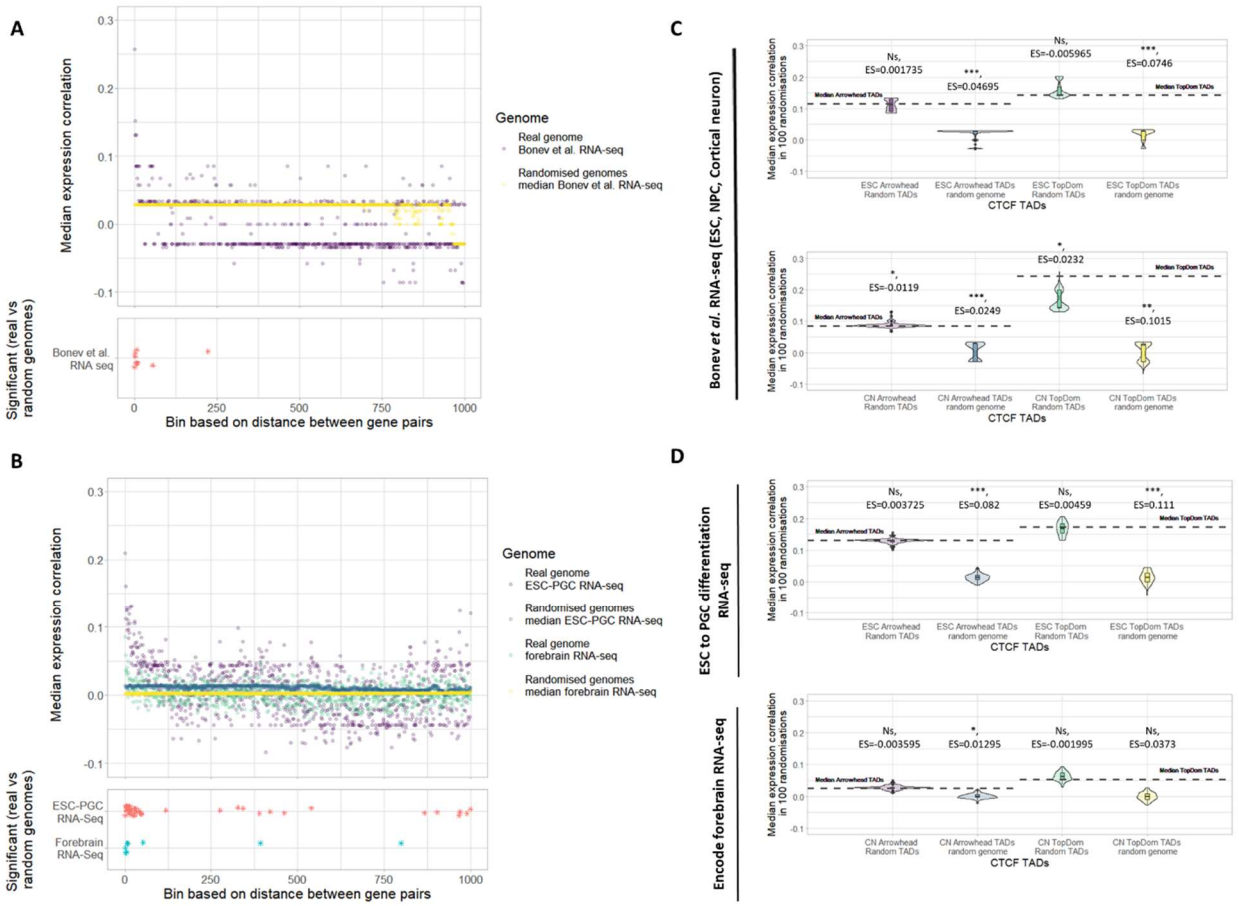

Figure 5: Pairwise gene co-expression in autosomal CTCF TADs. *Olfactory genes and paralogous gene pairs have been excluded in all panels. A-B) Top Panel: Median expression correlation coefficient (spearman) for pairs of genes vs binned distance in the real genome and 1000 random genomes. Bottom Panel: Stars indicate bins with a significantly higher median expression correlation in the real genome vs 1000 random genomes (FDR corrected p-value<0.05). Jitter has been applied on the y axis to allow clearer visualization of close together points. A) Expression correlation coefficients were calculated using RNA-seq from two replicates each of ESC, neural progenitor cells (NPC) and cortical neuron cells. B) Expression correlation coefficients were generated using mouse ESCs differentiating to primordial germ like cells (PGC) and forebrain RNA-seq from encode. The mouse ESCs differentiating to PGC RNA-seq was generated with three replicates each of ESCs, epiblast like cells (day 2), PGC (day 4) and PGC (day 6). The forebrain RNA-seq was generated with two replicates each, of embryos of varying ages. C-D) Median expression correlation coefficient (spearman) for pairs of genes in CTCF TADs (dotted line) and median expression correlation*

930 *coefficient (spearman) in 100 sets each of: random CTCF TADs and random genome CTCF TADs. CTCF*

931 *TADs called using both Arrowhead and TopDom, in both ESCs and cortical neurons (CN) Hi-C*

932 *(Wilcoxon test, Median p-value: p<0.001 = ***, p<0.01 = **, p<0.05 = *, NS= not significant, Median*

933 *ES= Effect size calculated using r for Wilcoxon). C) Expression correlation coefficients were calculated*

934 *using RNA-seq from A. D) Expression correlation coefficients were calculated using RNA-seq from B.*

935

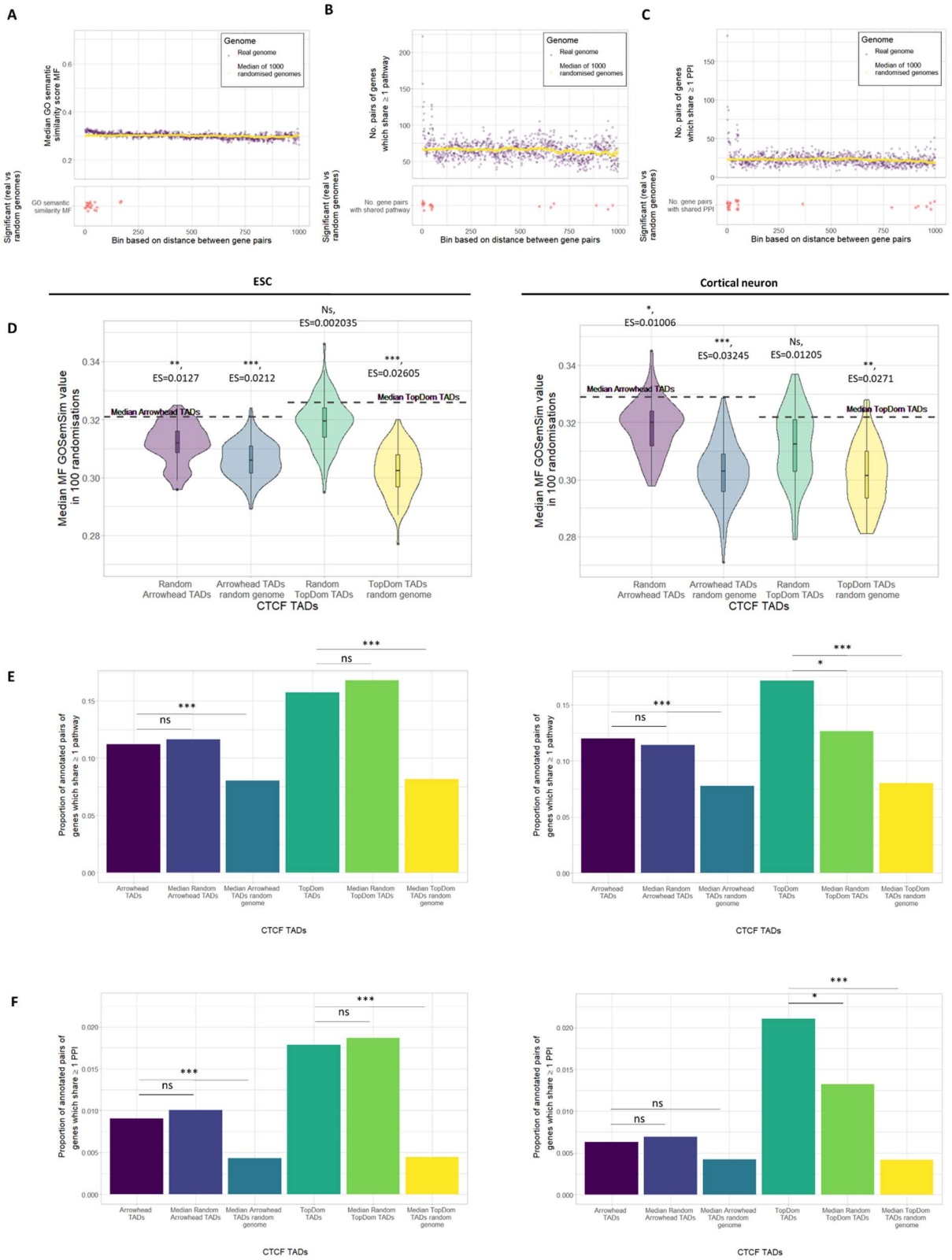

Figure 6: Functional similarity of pairs of genes in autosomal CTCF TADs. *Olfactory genes and paralogous gene pairs have been excluded in all panels. A-C) Top Panel: Median GO semantic similarity, number of shared pathways or number of shared PPI for pairs of genes vs binned distance*

*in the genome and 1000 random genomes. Bottom Panel: Stars indicate bins with a significantly higher functional similarity in the genome vs 1000 random genomes (FDR corrected p-value<0.05). D-F) TADs called using both Arrowhead and TopDom; in both ESC and cortical neuron Hi-C. Median P-value: p<0.001 = ***, p<0.01 = **, p<0.05 = *, NS= not significant. A) Distribution of MF GO semantic similarity for pairs of genes binned by distance in the genome vs 1000 random genomes. B) Distribution of the number of pairs of genes sharing ≥ 1 pathway binned by distance in the genome vs 1000 random genomes. C) Distribution of the number of pairs of genes sharing ≥ 1 PPI binned by distance in the genome vs 1000 random genomes. D) Median MF GO semantic similarity for pairs of genes in CTCF TADs (dotted line) compared to the distributions of median MF semantic similarity for 100 sets each of: random CTCF TADs and random genome CTCF TADs (Wilcoxon test, Median p-value, Median ES= Effect size calculated using r). E) Proportion of pairs of genes sharing ≥ 1 pathway in TADs and the median proportion of pairs of genes sharing ≥ 1 pathway in 100 sets each of: random CTCF TADs and random genome CTCF TADs (Fisher's exact test, Median p-value. F) Proportion of pairs of genes sharing ≥ 1 PPI in TADs and the median proportion of pairs of genes sharing ≥ 1 PPI in 100 sets each of: random CTCF TADs and random genome CTCF TADs (Fisher's exact test, Median p-value).*